

Density waves and jamming transition in cellular automaton models for traffic flow

L. Neubert^a, H.Y. Lee^b, M. Schreckenberg^a

^a *FB 10, Theoretische Physik, Gerhard-Mercator-Universität Duisburg, 47048 Duisburg, Germany*

^b *Dept. of Physics and Centre for Theoretical Physics, Seoul National University, Seoul 151-742, Korea*

Abstract

We present results of numerical investigations of the Nagel-Schreckenberg model, a microscopic traffic flow model based on a cellular automaton. This model exhibits a jamming transition with increasing vehicular density from a free-flow phase to a congested phase. The transition manifests in the behavior of the auto-correlation function which permits the determination of the velocity of upstream moving density waves. The numerical examinations are extended on two modifications of the standard cellular automaton, the slow-to-start model and the T² model. We investigate the jam velocity depending on several parameters and the auto-correlation function itself, we figure out the close interrelations between our measurements and the fundamental diagram of traffic flow and give a brief comparison with real traffic data.

I. INTRODUCTION

Recently, the examination and modeling of vehicular traffic became an important subject of research – see [1–6] and references therein for a brief review. In the microscopic approach to the traffic flow problem, the cellular automaton introduced in [7] reproduces important entities of real traffic, like the flow-density relation or stop-and-go waves. Beside the realization of some basic requirements to such a model it can be efficiently used in computational investigations and applications [8–10]. This is due to the simplicity of its rules. The simulation of real traffic as we know it by our daily experiences can be performed using multi-lane rules and vehicle- or road-dependent parameters [10,11]. Fundamental analytical and numerical examinations enclose exact solutions for certain limits and mean-field approximations [12–14], the jamming transition [15,16] or the effects of perturbations and the occurrence of metastable states [17–19], exemplary.

We investigate the density waves and the separation of the considered systems in free-flow and dense regions by the auto-correlation function. It enables us to trace back the spatiotemporal evolution of jams which are stable when a critical global density ρ_c is exceeded. It will be shown that the jamming transition is observable for varying both the global density ρ and the global noise p . The jam velocity can be derived directly from the auto-correlation function and closely related with the global flow-density relation (fundamental diagram). A

further subject of interest are modifications of the standard cellular automaton, but it will be proved that the explanations for the jam velocity are also applicable.

The present paper is arranged as follows: Section 2 is devoted to the explanation of the underlying model and two of its modifications. These modifications are characterized by a particular treatment of standing vehicles with regard to their headways. In section 3 we introduce our measurement methods. The auto-correlation function $C_{v_j}(r, \tau)$ is suitable to determine jam velocities and to estimate the critical density ρ_c as well as the critical noise p_c where stable density waves emerge. Furthermore, we will discuss the results of our numerical simulations with regard to the dependences on the global density and the maximum velocity, for instance. Concluding, we will give a short summary and verify the accordance with measurements on real traffic.

II. THE MODEL

Within the framework of this paper we only consider a one-dimensional ring of cells, each cell is 7.5 m long. The cells are either vacant or occupied by a vehicle labelled i . Its position is x_i and its discrete velocity is $v_i \in \{0, 1, \dots, v_{max}\}$. The gap g_i denotes the number of empty sites to its leading vehicle. The rules for a *parallel update* are

- Acceleration with regard to the vehicle ahead: $v_i \leftarrow \min(v_i + 1, g_i, v_{max})$,
- Noise: with a certain probability p do: $v_i \leftarrow \max(v_i - 1, 0)$,
- Movement: $x_i \leftarrow x_i + v_i$.

One time step corresponds to 1 sec, hence $\Delta v = 1$ in the simulation corresponds to $\Delta v = 7.5 \text{ m/s} = 27 \text{ km/h}$ in reality. These rules describe a spatially and temporally discrete model. The investigated systems consist of L cells and N vehicles, the global density is $\rho = N/L$. The flow is defined as $J = \langle v \rangle \rho$ with the mean velocity $\langle v \rangle = \sum v_i / N$. In the following this standard model is denoted with SCA.

We extend our studies on further modifications of the SCA, the *slow-to-start* model (STS) [18,19] and the T^2 model designed by Takayasu and Takayasu [20]. The modifications are as follows: For the STS velocity-depending deceleration probabilities $p(v_i)$ are employed with $\tilde{p}(v_i = 0) = \text{Min}(p + p_{STS}, 1)$, it is a special case among the VDR (=velocity depending rules) cellular automata models. Note that v_i is the velocity before the first update step is performed. In the T^2 model we distinguish between standing and moving vehicles: standing ones with a headway $g_i = 1$ only accelerate with a certain acceleration probability $1 - \tilde{p}$ with $\tilde{p} = \text{Min}(p + p_{T^2}, 1)$, whereas for all other ones the rules have been retained unchanged. Unlike the SCA with similar parameters, both models exhibit a different behavior in the vicinity of the point of maximum flow ($\rho_{max} \equiv \rho(J_{max}), J_{max}$). They are capable to generate metastable states in the adiabatic approach, i.e. one finds two branches of $J(\rho)$ in a small interval around ρ_{max} . One of them is the stable one, the other is characterized by its finite life times, hysteresis loops can be found. We summarize:

$$\begin{aligned}
\text{SCA: } & p = \text{const.} \\
\text{STS: } & \tilde{p} = \begin{cases} \text{Min}(p + p_{STS}, 1) & v_i = 0 \\ p & \text{otherwise} \end{cases} \\
\text{T}^2: & \tilde{p} = \begin{cases} \text{Min}(p + p_{T^2}, 1) & v_i = 0 \wedge g_i = 1 \\ p & \text{otherwise} \end{cases}
\end{aligned} \tag{1}$$

Actually, other definitions of \tilde{p} are conceivable, but, for our purpose, we decided to use only the above ones. Primarily, this had been done in order to model moving vehicles with similar properties and to scan the parameter space by varying only p , p_{STS} as well as p_{T^2} are of any value but fix.

III. SIMULATION RESULTS AND THEIR DISCUSSION

The density waves are moving upstream and can be easily observed in a space-time plot [7,21], one finds separation of dense and free-flow regions (Fig. 1). For the measurements it is necessary to introduce the mean local density of a cell k

$$\rho_k(t) \equiv \frac{1}{\lambda} \sum_{i=0}^{\lambda-1} \eta_{k+i} \quad \text{with} \quad \eta_{k+i} = \begin{cases} 1 & \text{if site } k+i \text{ is occupied} \\ 0 & \text{otherwise} \end{cases} \tag{2}$$

and an additional parameter λ that describes the length of the interval on which the local density has to be computed. It should satisfy the condition $\lambda_0 \ll \lambda \ll L$ [16] with a characteristic length scale λ_0 that is associated with the density fluctuations. On the other hand, one has to pay attention to the adjustment of the ratio λ/L in order to perform reliable simulations. For the determination of the jam velocity v_j we use the generalized T -point-auto-correlation function

$$C_{v_j}(r \equiv v_j^* \tau \Delta T, \tau) = \langle \prod_{\tau=0}^{T-1} \rho_k(x + v_j^* \tau \Delta T, t + \tau \Delta T) \rangle_L \tag{3}$$

with the supposed jam velocity $v_j^* \in [-1, 0]$. Among these v_j^* 's there is a value that develops $C_{v_j}(r, \tau)$ to the maximum. One has to scan the interval of all possible v_j^* 's until reaching the maximum of $C_{v_j}(r, \tau)$ – this is the desired real jam velocity v_j (Fig. 2). ΔT is the temporal distance between two single measurements which contributes to (3). Sufficiently large values of ΔT are necessary in order to observe a macroscopic motion and to determine v_j with an adequate accuracy. Unless otherwise mentioned, we set $L = 10^4$ and $\Delta T = 10^2$. We are averaging over 20 measurements. The choice of parameters ensures that any finite size effects are excluded.

The inset of Fig. 2 points out that one has to adjust thoroughly the parameters T and ΔT . When T is of the order of magnitude of ΔT or larger the error of estimating v_j screens the accuracy of the measurement, C_{v_j} vanishes and the determination of all depending quantities fails. This problem becomes more serious while approaching ρ_c . In this region the calculations are complicated additionally because of the large fluctuations of C_{v_j} itself.

The jam velocity v_j depends on the deceleration probability as it can be seen in Fig. 3 and is related to global quantities as it can be shown later. We checked it for a variety of parameters, but could not notice any remarkable deviations among the diverse sets of data. The modifications of the SCA, the STS and the T^2 , yield a different behavior, a small sample is also instanced in Fig. 3. The absolute values of the jam velocity in the models STS and T^2 are smaller than that of the SCA. This implies that both modifications are characterized by a lowered outflow from a jam that, in turn, reduces the jam velocity.

The results of simulations using the STS are basically shifted towards smaller $|v_j|$'s and proportional to p_{STS} , concurrent with increasing p_{STS} the function $v_j(p)$ becomes more and more linear (Fig. 3). Note that it is set $p_{STS} = \{0.3|0.5\}$. p_{STS} can be recognized on the ordinate at $p = 0$ and on the abscissa at $v_j = 0$, for large volumes of p a total deadlock occurs. In order to find out how v_j is related to \tilde{p} we investigate the mean waiting time t_w for $\tilde{p} < 1$ which can be approached by a infinite series:

$$t_w = 1(1 - \tilde{p}) + 2(1 - \tilde{p})\tilde{p} + 3(1 - \tilde{p})\tilde{p}^2 + \dots = (1 - \tilde{p}) \sum_{n=1}^{\infty} n\tilde{p}^{n-1} = \sum_{n=0}^{\infty} \tilde{p}^n. \quad (4)$$

That, in turn, directly leads to an estimation of the jam velocity:

$$|v_j| = \frac{1}{t_w} = 1 - \tilde{p} \in [0, 1 - p_{STS}], \quad (5)$$

since it is always $\tilde{p} = \text{Min}(p + p_{STS}, 1)$. (5) is exact for $p = 0$, and for large p_{STS} one obtains a good agreement with the simulations results (Fig. 3). As known from space-time plots of SCA simulations, so-called subjams emerge in front of the major jam, they reduce $|v_j|$. The ansatz (4) is made without regard to this fact, hence we overestimate $|v_j|$, mainly for small p_{STS} .

The results drawn from simulations using the T^2 model obey no deadlock situation for any $p < 1$. Starting from $p = 1$, one can hardly distinguish between SCA and T^2 . Especially, this is valid for approximately $p_{T^2} > 1 - p$, i.e. the Minimum-function in (1) operates resp. it has a significant effect on the considered scenario. Now, a derivation for the waiting time similar to (4) should be attempted:

$$t_w = 1(1 - \tilde{p}) + 2(1 - p)\tilde{p} + 3(1 - p)\tilde{p}p + 4(1 - p)\tilde{p}p^2 + \dots = 1 + \tilde{p} \sum_{n=0}^{\infty} p^n \rightsquigarrow \frac{1 - p + \tilde{p}}{1 - p}. \quad (6)$$

But soon some heavy problems arise: For small p_{T^2} the jam velocity is overestimated for all values of p , which, in turn, can be traced back to the occurrence of subjams. With increasing p_{T^2} even for small p it is required to incorporate the Minimum-function in (1). Again, it is $|v_j| = t_w^{-1}$ and according to (6) the estimations of two special cases can be tried and verified by Fig. 3:

$$|v_j|(p = 0) = \frac{1}{1 + p_{T^2}} \quad \text{and} \quad |v_j|(p_{T^2} \approx 1) = \frac{1 - p}{2 - p}. \quad (7)$$

Obviously, the measurements are strongly affected by the global vehicular density ρ . Below ρ_c the vehicles moves almost freely and independent of each other, i.e. there is no

correlation between them. For $\rho \geq \rho_c$ one finds upstream moving density waves which can be recognized by (3). In the vicinity of ρ_c the jam velocity reveals large fluctuations (Fig. 4), otherwise it could be assumed to be constant. Within the range where density waves are to be expected it is obviously that v_j is independent of ρ . This is originated in the independence between the outflow from a jam and the global density. Near ρ_c many jams emerge and disappear again within a few time, which causes causes the large fluctuations. We also find only a very weak dependence between v_j and v_{max} provided that v_{max} is sufficiently large (Fig. 5). For smaller quantities than depicted in Fig. 5 the measurements are negatively influenced by the relatively high probability of vehicles with $v = 0$, i.e. it is more likely that vehicles halt, but do not cause a stable jam.

Up to now we applied the auto-correlation function (3) to determine the jam velocity. But this quantity itself indicates the two different phases separated by a critical deceleration probability p_c (Fig. 6) or by a critical density ρ_c (Fig. 7). Varying p leads to a transition while crossing p_c . Its clarity strongly depends on $T/\Delta T$, for insufficient ratios a plateau at $\bar{C}_{v_j}(p)$ occurs. The modified auto-correlation \bar{C}_{v_j} used here is defined as

$$\bar{C}_{v_j}(r, \tau) = \left\langle \left(\prod_{\tau=0}^{T-1} \rho_k(x + v_j^* \tau \Delta T, t + \tau \Delta T) \right)^{1/T} \right\rangle_L \quad (8)$$

and has the dimension of density *veh/site*. The other transition takes place while crossing the density ρ_c . From a formal point of view it can be written as $C_{v_j}(\rho) = f(\rho) \Theta(\rho - \rho_c)$ with the heavy side function Θ and a certain $f(\rho)$ that reflects the density dependence for $\rho > \rho_c$ (Fig. 7). For $\rho < \rho_c$ one finds empty regions of the order of magnitude of λ , and therefore C_{v_j} completely vanishes. While approaching ρ_c with an too large ratio λ/L a finite C_{v_j} renders only the possibility to find vehicles within λ and does not refer to a density wave. Thus, only a small λ/L allows the estimation of ρ_c . On the other hand, for $\rho > \rho_c$ stable congestion emerge. The centroid of the same jam can be detected at $t_i = 0$ as well as at $t_f = \tau \Delta T$ located at $x(t_i) - |v_j| t_f$. Its higher density crucially contributes to C_{v_j} which remains finite during the whole simulation. In this context, ρ_c can be denoted as the density, at which long-term or never-ending jams emerge. It separates the densities as to be seen in the inset of Fig. 7 with the modified auto-correlation $\bar{C}_{v_j}(\rho)$ (8). For a fixed density and a varying v_{max} the relationship can be estimated as $C_{v_j}(v_{max}) \propto \rho$ (Fig. 8). Nevertheless, the quality of these data does not allow a correct classification of the transition between the free-flow and the dense region. Above all, the sensitive dependencies on the many adjustable parameters of this measurement method seem to prevent a more accurate consideration of the interesting range of density.

How is the jam velocity related to other macroscopic quantities? In the steady state recognized by a conserved number and length of jams the dynamics are characterized by an equilibrium of out-flowing vehicles and vehicles attaching the jam from behind. The more frequent vehicles join the jam the faster the jam moves upstream. If we neglect any effects due to metastability then the free-flow region can be assumed to be located in the vicinity of the point of maximum flow (ρ_{max}, J_{max}). Hence, the velocity of attaching vehicles is on average $\langle v_{att} \rangle = J_{max}/\rho_{max}$. The mean distance between the tail of the jam and the next vehicle is $\langle g \rangle = \rho_{max}^{-1} - 1$. It directly leads to the temporal distance

$$\Delta t_{att} = \frac{\langle g \rangle}{\langle v_{att} \rangle} \Leftrightarrow v_j = \frac{J_{max}}{\rho_{max} - 1} \leq 0. \quad (9)$$

This is confirmed by the simulation results depicted in Fig. 9. It means that v_j is determined by the slope of the congested branch ($\rho \geq \rho_{max}$) in the fundamental diagram. This can also be verified for the modifications STS and T^2 (Fig. 10). The small deviations from the data drawn from simulations rest upon a difference between the outflow of the jam and the maximum global flow in the considered systems, but also in the above made assumption of the equilibrium. Actually, the lowered outflow from jams observed in the models STS and T^2 in comparison to the SCA is also reflected by (9).

Concluding, this knowledge enables a calibration of the SCA. Besides the approach of the fundamental diagram derived from empirical data a further point of interest is the velocity of upstream moving jams ($\approx -15 \text{ km/h}$ on German highways [22]) – but according to (9) all information is accumulated in the fundamental diagram, namely in the second characteristic slope of $J(\rho)$. Exemplary, for the SCA it is set $v_{max} = 5$ and $p = 0.2 \cdots 0.3$ to adapt the simulation to this empirical jam velocity.

IV. SUMMARY

We investigated the cellular automaton model for vehicular traffic in order to get information about the density waves and the velocity of their centroids. Beside the standard cellular automata SCA we also included two of its modifications, the *slow-to-start* model STS and the T^2 model. Both resemble the SCA except the rules for standing vehicles. Loosely spoken, they result in a lower flow downstream a jam. For the determination of the jam velocity and behavior of the model nearby the critical density ρ_c we used the auto-correlation function $C_{v_j}(r, \tau)$. Despite the high computational efforts ($\mathcal{O}(L^2)$) this method was suitable to be applied for our calculations.

The quantity $C_{v_j}(r, \tau)$ reflects the two different phases and depends on the global density ρ . The density regime is separated by the critical density ρ_c . For $\rho < \rho_c$ stable jams cannot be detected by the applied method, whereas for larger ρ the system is dominated by sequences of dense and free-flow regions, where C_{v_j} remains finite and permits an estimation of ρ_c . At this point a crossover to the congested region takes place. Both the local length λ and the number of calculations T have large influence on C_{v_j} . Further statements regarding the transition cannot be given due to the numerical insufficiencies and accuracy.

Additionally, the correlation function includes information about the jam velocity. For sufficiently large ρ the absolute value of v_j is a continuous and descending function of p , but depends on the model under consideration. The differences between the models, especially for $p \rightarrow 0$ and partially $p \rightarrow 1$, could be explained phenomenologically by waiting time arguments. The jam velocity is essentially determined by the point (ρ_{max}, J_{max}) in the fundamental diagram, irrespective of the considered model.

REFERENCES

- [1] D.E. Wolf, M. Schreckenberg and A. Bachem (eds.), *Traffic and Granular Flow* (World Scientific, Singapore, 1996).
- [2] M. Schreckenberg and D.E. Wolf (eds.), *Traffic and Granular Flow* (Springer, Singapore, 1998).
- [3] M.J. Lighthill and G.B. Whitham, in *Proc. Roy. Soc. of London A*, ed. by C. Herring (Cambridge, 1955), p. 281.
- [4] B.S. Kerner and P. Konhäuser, Phys. Rev. E **48** 4, 2335 (1993).
- [5] M. Bando, K. Hasebe, A. Nakayama, A. Shibata and Y. Sugiyama, Phys. Rev. E **51** 2, 1035 (1995).
- [6] D. Helbing, Phys. Rev. E **55** 3, 3735 (1997).
- [7] K. Nagel and M. Schreckenberg, J. de Phys. I **2**, 2221 (1992)
- [8] B. Chopard, P.O. Luthi and P.A. Queloz, J. Phys. A **29**, 2325 (1996).
- [9] M. Rickert and K. Nagel, Int. J. of Mod. Phys. C **7** (1996).
- [10] J. Esser, M. Schreckenberg, Int. J. of Mod. Phys. C **8** 5, 1025 (1997).
- [11] P. Wagner, K. Nagel and D.E. Wolf, Physica A **234**, 687 (1997).
- [12] A. Schadschneider and M. Schreckenberg, J. Phys. A **26**, L679 (1993).
- [13] A. Schadschneider and M. Schreckenberg, J. Phys. A **30**, L69 (1997).
- [14] A. Schadschneider and M. Schreckenberg, J. Phys. A **31**, L225 (1998).
- [15] B. Eisenblätter, L. Santen, A. Schadschneider and M. Schreckenberg, Phys. Rev. E **57** 2, 1309 (1998).
- [16] S. Lübeck, M. Schreckenberg and K.D. Usadel, Phys. Rev. E **57** 1, 1171 (1998).
- [17] S. Krauß, P. Wagner and C. Gawron, Phys. Rev. E **55** 5, 5597 (1997).
- [18] A. Schadschneider, M. Schreckenberg, Ann. Physik **6**, 541 (1997).
- [19] R. Barlovic, L. Santen, A. Schadschneider, M. Schreckenberg, Euro. Phys. Journal B (accepted for publication) (1998).
- [20] M. Takayasu and H. Takayasu, Fractals **1**, 860 (1993).
- [21] J. Treiterer, Ohio State University Technical Report No. PB 246094, Columbus Ohio (1975).
- [22] B.S. Kerner and H. Rehborn, Phys. Rev. E **53** 2, R1297 (1996).

FIGURES

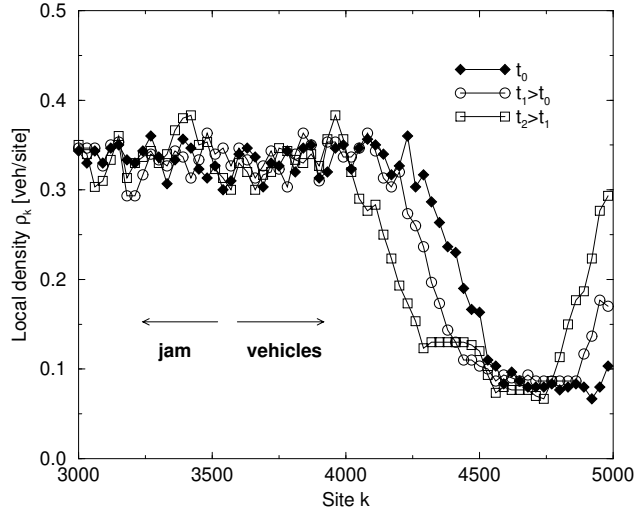


FIG. 1. Temporal evolution of the local density in the SCA – jam fronts and vehicles are moving in opposite directions. It is set $v_{max} = 5$, $p = 0.5$ and $\lambda = 50$.

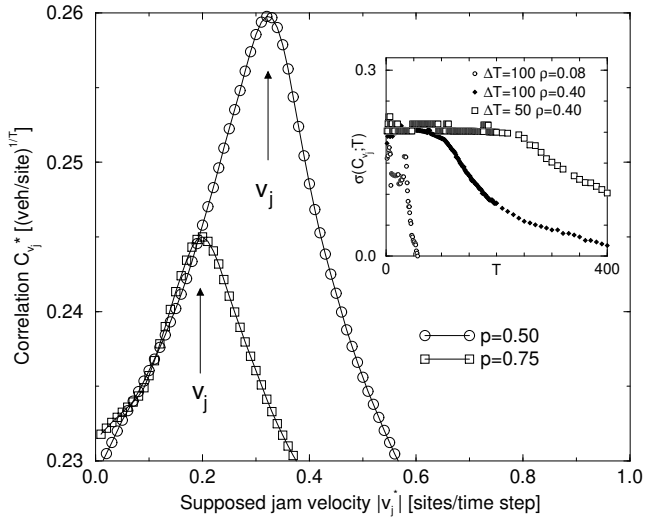


FIG. 2. The peak of the correlation function enables to estimate the jam velocity v_j ($v_{max} = 5$, $\lambda = 50$ and $\rho = 0.4$). The standard deviation of the symmetrically assumed C_{v_j} is depicted in the inset. For certain ratios $T/\Delta T$ the variance shrinks a lot. For an improper relationship the correlation function vanishes and inhibits the estimation of further quantities. In the vicinity of ρ_c this sensitivity is more pronounced and complicates the calculations. On the other hand, for shrinking ΔT the function C_{v_j} is significantly broadened and therefore its variance σ is higher.

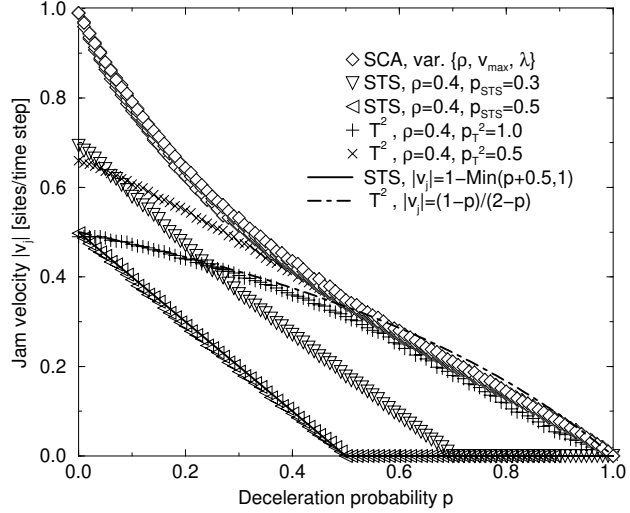


FIG. 3. The jam velocity as a function of the deceleration probability depends on the considered model. The results of the SCA using various parameters and that of STS and T^2 differ obviously, the error bars are within the symbol size. Note that $v_{max} = 5$ and $\lambda = 30$ is set for STS and T^2 , whereas the choice of v_{max} does not influence the results for all models.

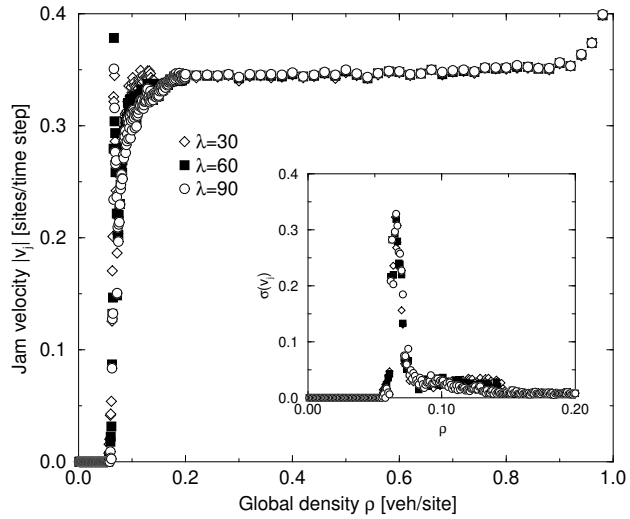


FIG. 4. Plot of $v_j(\rho)$ for $v_{max} = 5$, $p = 0.5$. Beyond ρ_c , especially for $0.2 \leq \rho \leq 0.8$, $v_j(\rho)$ can be assumed to be constant. The inset reveals the large fluctuations of v_j nearby ρ_c which are up to the order of magnitude of v_j itself.

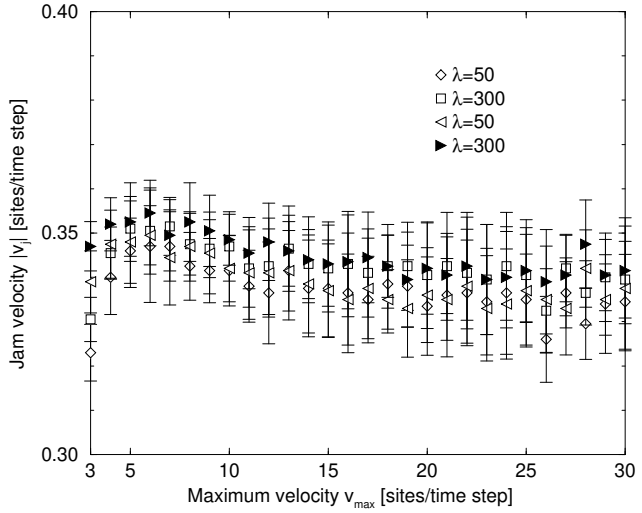


FIG. 5. Plot of $v_j(v_{max})$ for fixed ρ and $v_{max} = 5$, $p = 0.5$. The data are located within the error bars quite well. They are weakly descending according to the fact that the maximum flow J_{max} depends on v_{max} .

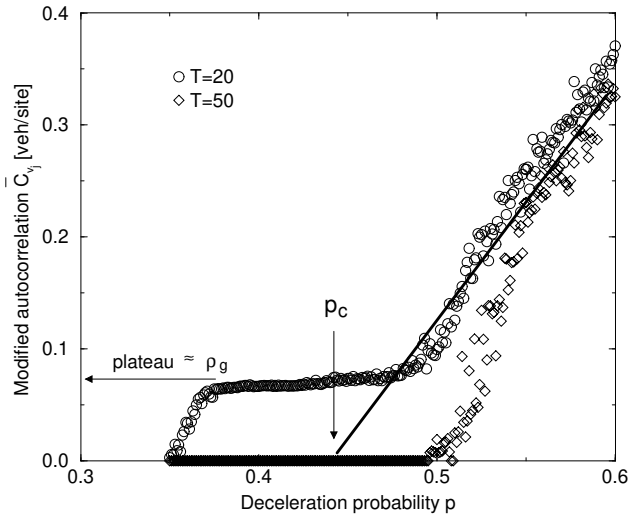


FIG. 6. The transition can also be obtained by varying the deceleration probability p ($v_{max} = 5$). Here, the transition is smeared out due to finite size effects and systematic errors in the determination of \bar{C}_{v_j} (8). For small T a plateau at $\bar{C}_{v_j} = \rho_g$ can be identified near ρ_c . $\rho = 0.073$, $v_{max} = 5$ and $\lambda = 30$ are employed for both data sets, T varies.

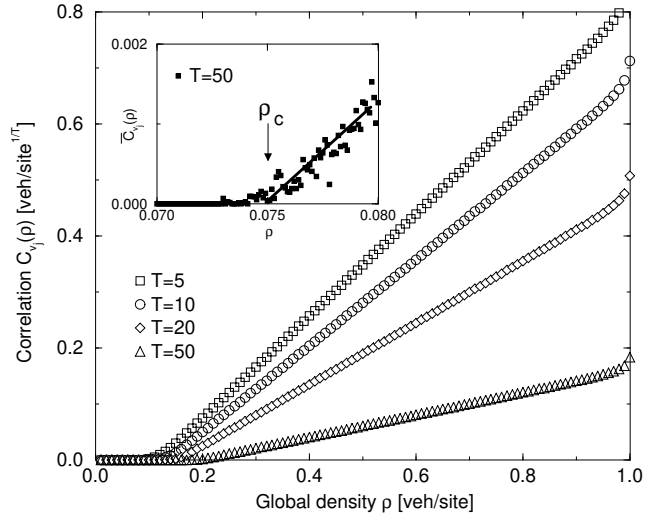


FIG. 7. Plot of the the auto-correlation function $C_{v_j}(\rho)|_{v_{max}}$ for $v_{max} = 5$, $p = 0.5$ and $\lambda = 30$. Below a signified density the correlation function vanishes due to the absence of stable jams. The inset zooms into the region $\rho \approx \rho_c$ for the modified auto-correlation $\bar{C}_{v_j}^{1/T}$ (8). As suggested by other results not published here that too large ratios λ/L broadens the transient region.

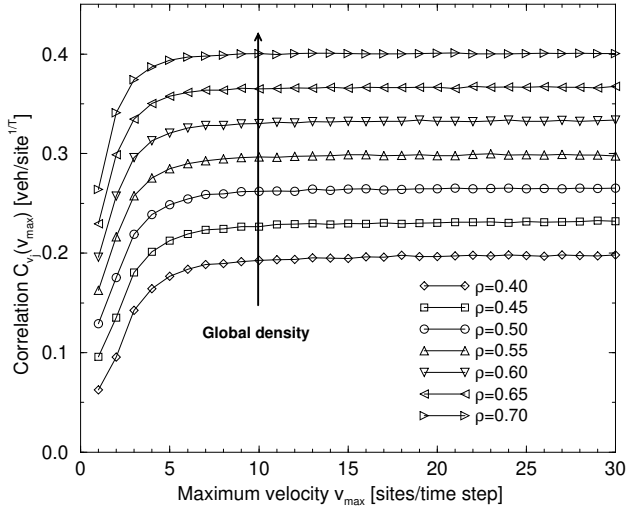


FIG. 8. Plot of the the correlation function $C_{v_j}(v_{max})|_{\rho}$ for $p = 0.5$ and $\lambda = 30$. A explanation similar to $v_j(v_{max})$ can be applied in order to discuss $C_{v_j}(v_{max})|_{\rho}$, but, in addition, there is a simple linear relationship between C_{v_j} and ρ .

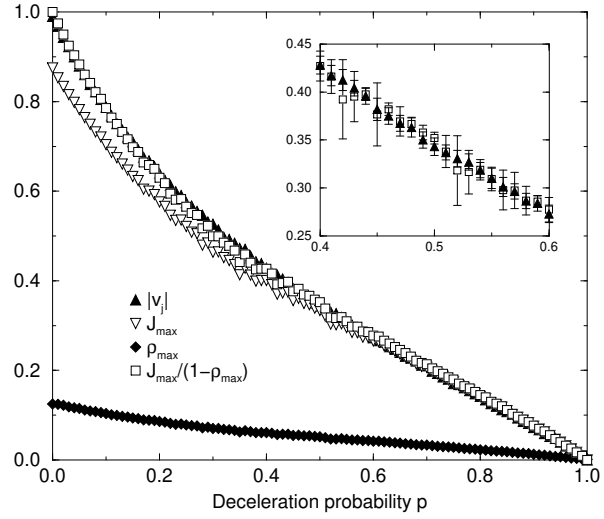


FIG. 9. The jam velocity can be explained by (9): $v_j = J_{max}/(\rho_{max} - 1)$ – a consequence of the phase separation for $\rho > \rho_c$. As shown in the inset, the data agree within the error bars, i.e. the jam velocity is directly related to the slope of the congested branch of a fundamental diagram ($v_{max} = 5$, $p = 0.5$ and $\lambda = 30$).

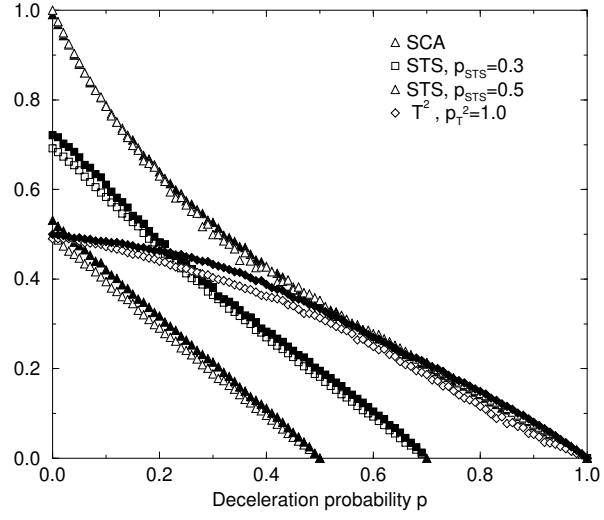


FIG. 10. v_j (filled symbols) for all used models ($v_{max} = 5$, $\lambda = 30$) are depicted as well as $J_{max}/(\rho_{max} - 1)$ (opaque symbols). The small deviations are related to the discrepancies between the outflow of a jam and the global maximum flow.